Dynamic Compartmentalization of Bacteria: Accurate Division in *E. Coli*

Martin Howard,[1,*] Andrew D. Rutenberg,[2] and Simon de Vet[2]

[1]*Department of Physics, Simon Fraser University, Burnaby, British Columbia, Canada V5A 1S6*
[2]*Department of Physics, Dalhousie University, Halifax, Nova Scotia, Canada B3H 3J5*

(Received 14 July 2001; published 10 December 2001)

Positioning of the midcell division plane within the bacterium *E. coli* is controlled by the *min* system of proteins: MinC, MinD, and MinE. These proteins *coherently* oscillate from end to end of the bacterium. We present a reaction-diffusion model describing the diffusion of *min* proteins along the bacterium and their transfer between the cytoplasmic membrane and cytoplasm. Our model spontaneously generates protein oscillations in good agreement with experiments. We explore the oscillation stability, frequency, and wavelength as a function of protein concentration and bacterial length.

DOI: 10.1103/PhysRevLett.87.278102 PACS numbers: 87.17.Ee, 87.16.Ac, 82.39.Rt

The subcellular spatial and temporal organization of bacterial proteins is largely unknown. Already, the spatial distribution of proteins on the cytoplasmic membrane of bacteria are known to be important for chemotaxis [1] and for DNA replication [2]. Improving our understanding of how this supramolecular organization of proteins affects bacterial function represents a considerable experimental and theoretical challenge. In contrast to nucleated eukaryotic cells, no large organelles are present in the bacterial interior (cytoplasm), and no active transport mechanisms such as molecular motors are known to function there. However, recent video microscopy of fluorescently labeled proteins involved in the regulation of *E. coli* division have uncovered coherent and stable spatial and temporal *oscillations* in three proteins: MinC, MinD, and MinE [3–8]. The proteins oscillate from end to end of the bacterium, and move between the cytoplasmic membrane and the cytoplasm. These *min* proteins select the site for the next bacterial division [9,10]. Despite a wealth of phenomenological detail, no quantitative models have been developed of how the *min* proteins organize into oscillating structures. Understanding the self-organized patterns involved in bacterial division processes can give us insight into how a bacterium can dynamically compartmentalize itself.

We focus on *E. coli*, a commonly studied rod shaped bacterium, approximately $2-6\ \mu$m in length and around $1-1.5\ \mu$m in diameter. Each *E. coli* divides roughly every hour, depending on the conditions — first replicating its DNA then dividing in half to form two viable daughter cells. The MinCDE oscillations are known to persist even when protein synthesis is suppressed [3], and DNA replication and septation occur even without the *min* proteins. Hence, the *min* system can be studied independently of the other division processes. Efficient division requires many processes, including DNA replication, MinCDE oscillations, and the actual septation process. Septation initiates with a contractile polymeric "Z-ring" of a tubulin-homologue FtsZ that forms just underneath the cytoplasmic membrane. The FtsZ septation rings largely avoid guillotining the DNA-containing nucleoids independently of the *min* system [11]. This "nucleoid occlusion" serves as a complementary control mechanism for accurate cell division. The role of the *min* system appears to be to restrict the Z-ring to midcell. This reduces the production of inviable nucleoid-free minicells which occur when the cell divides too close to the cell poles. If the *min* system is genetically knocked out, 40% of the divisions lead to inviable minicells [9]—a sizable drain on bacterial resources.

The study of deletion mutants has made the phenomenological roles of the individual *min* proteins clear. MinC associated to the cytoplasmic membrane locally inhibits assembly of the contractile Z-ring, but remains cytoplasmic and largely inactive in the absence of MinD [5]. MinD binds MinC and recruits it to the cytoplasmic membrane [5,12]. MinE drives MinD away from the bacterial midplane, and, hence, allows a contractile ring to form only there. Without MinE, the membrane-bound MinC/MinD block Z-ring formation everywhere, inhibiting division, and resulting in the formation of long filamentous cells [4,6]. Without MinC, Z-ring formation cannot be inhibited anywhere and inviable minicells are produced. Without MinD, neither MinC nor MinE are recruited to the cytoplasmic membrane and so have a reduced effect.

With normal levels of MinC, MinD, and MinE, a remarkable oscillatory dynamics is seen [3–8]. First, the MinC/MinD accumulate at one end of the bacterium on the cytoplasmic membrane. Then MinE forms a band at midcell which sweeps towards the cell pole occupied by the MinC/MinD, ejecting the MinC/MinD into the cytoplasm as it goes. The ejected MinC/MinD then rebinds at the other end of the bacterium. When the MinE band reaches the cell pole, it disassociates and reforms at midcell. The entire process then repeats towards the opposite cell pole. The oscillation period is approximately 1–2 min, so many oscillations occur between each bacterial division. The dynamics minimizes the MinC/MinD concentration at midcell, thereby allowing the Z-ring and the subsequent division septum to form there.

Until recently [8], qualitative models of the *min* system involved unidentified midcell topological markers (see, e.g., [13]). This Letter puts forward the first quantitative

self-organized model that describes much of the intricate phenomenology of accurate division site placement in *E. coli*, and does so using *only* the diffusive motion and interactions of the *min* proteins. The essence of our approach is to describe the MinCDE dynamics by a set of coupled reaction-diffusion equations. Experimental results indicate that the oscillatory protein dynamics is unaffected if new protein synthesis is blocked [3]. Accordingly, we employ a model that conserves the total number of each protein type. Strikingly, this model possesses a linear Turing-like (Hopf) instability [14,15] despite the absence of mechanisms such as internal reactant production or external feed that have normally been required to model Turing patterns [16]. [Of course energy input in the form of adenosine triphosphate (ATP) is required to sustain the oscillations within a bacterium.] As we will see, the resulting protein oscillations mark the midcell with a minimum of the time-averaged concentration of MinC/MinD and with a corresponding maximum of MinE.

Our starting point is a set of four coupled reaction-diffusion equations describing, respectively, the densities of MinD on the cytoplasmic membrane (ρ_d), MinD in the cytoplasm (ρ_D), MinE on the cytoplasmic membrane (ρ_e), and MinE in the cytoplasm (ρ_E):

$$\frac{\partial \rho_D}{\partial t} = D_D \frac{\partial^2 \rho_D}{\partial x^2} - \frac{\sigma_1 \rho_D}{1 + \sigma_1' \rho_e} + \sigma_2 \rho_e \rho_d , \quad (1)$$

$$\frac{\partial \rho_d}{\partial t} = \frac{\sigma_1 \rho_D}{1 + \sigma_1' \rho_e} - \sigma_2 \rho_e \rho_d , \quad (2)$$

$$\frac{\partial \rho_E}{\partial t} = D_E \frac{\partial^2 \rho_E}{\partial x^2} - \sigma_3 \rho_D \rho_E + \frac{\sigma_4 \rho_e}{1 + \sigma_4' \rho_D} , \quad (3)$$

$$\frac{\partial \rho_e}{\partial t} = \sigma_3 \rho_D \rho_E - \frac{\sigma_4 \rho_e}{1 + \sigma_4' \rho_D} . \quad (4)$$

Following the observation in Refs. [4,5] that the MinC dynamics simply follows that of the MinD, we do not model the MinC field explicitly. We consider the variation of density along the long bacterial axis, tracking the local rates of change of the densities stemming from diffusion and from transfer between the cytoplasmic membrane and the cytoplasm. Zero flux "closed" boundary conditions are imposed at both ends of the bacterium. The total amount of MinD and MinE, obtained by integrating $\rho_d + \rho_D$ and $\rho_e + \rho_E$ over the length of the bacterium, is explicitly conserved by our dynamics.

By reducing the *min* protein dynamics to a set of deterministic $1d$ rate equations, we neglect fluctuation effects. Given that the number of *min* molecules in each cell is rather small (around 3000 for MinD [17] and 170 for MinE [18]), these fluctuations could be important. While some fluctuation effects are evident experimentally, such as an occasional midcycle reversal of the direction of MinE band propagation [8], on the whole bacterial oscillations appear to be amazingly regular [5]. Our continuum coarse-grained approach captures the essence of the protein dynamics and explains the self-organized aspects of the MinCDE oscillations.

In the first reaction terms in Eqs. (1) and (2), σ_1 describes the spontaneous association of MinD to the cytoplasmic membrane [6]. MinD is required to recruit MinE to the cytoplasmic membrane, but it is an open question whether it is cytoplasmic MinD or membrane-bound MinD that is primarily active. A cytoplasmic interaction between MinD and MinE has been observed in Ref. [12], and we are currently able to obtain the MinCDE oscillations only by allowing cytoplasmic MinD to recruit cytoplasmic MinE to the membrane, via σ_3 in Eqs. (3) and (4). Once on the membrane, MinE drives MinD into the cytoplasm. We represent this with σ_2 in the second reaction terms in Eqs. (1) and (2). Finally, MinE will spontaneously disassociate from the membrane, corresponding to σ_4 in the second reaction terms in Eqs. (3) and (4). We have not included spontaneous MinD disassociation or spontaneous MinE association terms, since experimentally MinE dominates the MinD disassociation and MinD dominates the MinE association.

Many other reaction terms are possible; however, we include only the simplest possible "renormalizations" of the basic recruitment and release terms, σ_1' and σ_4'. Effectively, σ_1' corresponds to membrane-bound MinE suppressing the recruitment of MinD from the cytoplasm, and σ_4' corresponds to cytoplasmic MinD suppressing the release of membrane-bound MinE. We have also set the diffusion constants for the membrane-bound MinD and MinE to zero. Our results are not qualitatively changed by using nonzero values, provided the membrane diffusion constants remain much less than their bulk counterparts.

For our simulations we discretized space and time with spacings of $dx = 8 \times 10^{-3}$ μm and $dt = 1 \times 10^{-5}$ s. We have checked that our results are unchanged with smaller dx and dt. Densities are measured in molecules per micron, and, unless otherwise stated, we use average densities of 1500 μm^{-1} for MinD [17] and 85 μm^{-1} for MinE [18]. The numerical values of our other parameters have not been experimentally determined for the *min* proteins. We choose cytoplasmic diffusion constants slightly less than the value 2.5 $\mu\text{m}^2\, s^{-1}$ directly measured for a maltose binding protein [19] in the *E. coli* cytoplasm. Unless otherwise mentioned, we use a length of 2 μm and the following values for the parameters in Eqs. (1)–(4): $D_D = 0.28$ $\mu\text{m}^2/\text{s}$, $D_E = 0.6$ $\mu\text{m}^2/\text{s}$, $\sigma_1 = 20$ s^{-1}, $\sigma_1' = 0.028$ μm, $\sigma_2 = 0.0063$ $\mu\text{m/s}$, $\sigma_3 = 0.04$ $\mu\text{m/s}$, $\sigma_4 = 0.8$ s^{-1}, and $\sigma_4' = 0.027$ μm.

We have analyzed the linear stability of Eqs. (1)–(4) [15]. Testing solutions of the form $e^{\lambda t + iqx}$ with the above parameter values, we find a complex $\lambda(q)$ with a positive real part that is maximized for $q \approx 1.5$ μm^{-1}, where $\lambda_{\text{max}} = 0.010 \pm 0.043i$. This indicates the presence of a maximally linearly unstable oscillating mode with a wavelength of 4.2 μm and a period of 145 s. This finding is confirmed by a direct numerical stability analysis of our

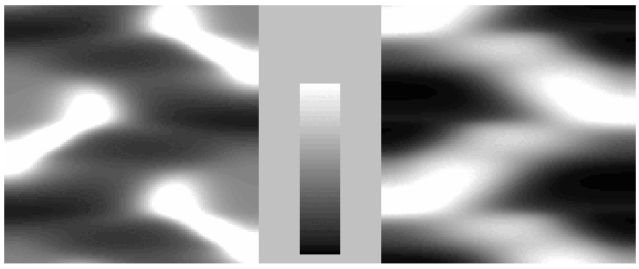

FIG. 1. Space-time plots of the total MinD (left) and MinE (right) densities. The grey scale runs from 0.0 to 2.0 times the average density of MinD or MinE, respectively. The MinD depletion from midcell and the MinE enhancement at midcell are immediately evident. Time increases from top to bottom, and the pattern repeats indefinitely as time increases. The grey-scale reference bar spans 100 s. The horizontal scale spans the bacterial length (2 μm).

model (not shown). The physical origin of this instability lies in the disparity between the membrane and cytoplasmic diffusion rates, and also in the slower rate at which MinE disassociates from the membrane. This ensures that the MinE dynamics lags that of the MinD, setting up the oscillating patterns. The existence of the linear instability in Eqs. (1)–(4) is crucial, since it means that the oscillating pattern will spontaneously generate itself from a variety of initial conditions—including nearly homogeneous ones. In our simulations, we used random initial conditions, although identical patterns were also observed with asymmetric initial distributions of MinD and MinE. The eventual oscillating state is stabilized by the nonlinearities in Eqs. (1)–(4). At the midcell, this oscillating pattern has a minimum of the time-averaged MinD concentration—an essential feature of division regulation—and a maximum of the time-averaged MinE concentratio.

Space-time plots of the MinD and MinE concentrations for a cell length of 2 μm are shown in Fig. 1. In excellent agreement with the experimental results, the MinE spontaneously forms a single band at midcell which then sweeps towards a cell pole, displacing the MinD, which then reforms at the opposite pole. Once the MinE band reaches the cell pole it disappears into the cytoplasm, only to reform at midcell where the process repeats, but in the other half of the cell. These patterns are stable over at least 10^9 iterations (10^4 s)—long enough for the *min* system to regulate cell division throughout the division cycle of the cell. In Fig. 2, we plot the time-averaged MinD and MinE densities as a function of position. MinD shows a pronounced dip in concentration close to midcell, which allows for the removal of division inhibition at midcell. This is in qualitative agreement with the experimental data of Ref. [8]. MinE peaks at midcell, with a minimum at the cell extremities.

We also investigated longer filamentous bacteria and found a multiple MinE band structure (not shown). Multiple MinE bands always combined into a single MinE band in cell lengths shorter than the natural wavelength indicated by linear stability analysis.

The oscillation period as a function of the average MinD concentration is shown in Fig. 3 (left). We find a linear relationship indicated by the best-fit line, where the period approximately doubles as the MinD concentration is quadrupled. A linear relationship has also been suggested experimentally [3]. The period of oscillation as a function of cell length is shown in Fig. 3 (right). Below lengths of 1.2 μm the bacterium does not sustain oscillating patterns. For lengths above this minimum, the oscillation patterns are stable and the period increases with length—as observed experimentally [7]. The periods measured from our numerics for cell lengths of 2 μm are around 100 s, in good agreement with experiments, where periods from 30–120 s have been found [3]. A single MinE band state is stable over a wide range of lengths for a given density of *min* proteins. This provides strong evidence that the *min* system is capable of regulating accurate cell division over normally occurring cell lengths as the cell grows between division events. At longer lengths of around 6 μm, we observe long-lived metastable states with two MinE bands. These multiple bands can survive for a thousand seconds or more before decaying into a single band. At still longer lengths the two band state appears stable; this occurs around 8.4 μm—twice the dominant wavelength given by the linear stability analysis. This explains why the characteristic wavelength of linear stability analysis is rather longer than a normal *E. Coli* bacterium—if the length scale were smaller, then multiple MinE bands might

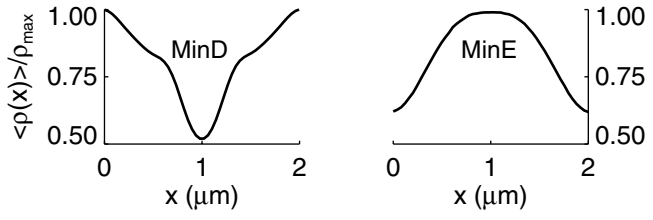

FIG. 2. The time-average MinD (left) and MinE (right) densities, $\langle \rho(x) \rangle / \rho_{\max}$, relative to their respective time-average maxima, as a function of position x (in μm) along the bacterium.

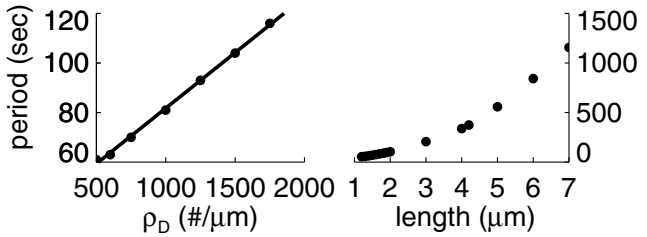

FIG. 3. Left: Plot of the period of oscillation (in seconds) against MinD density (in μm^{-1}), at fixed average MinE concentration of 85 μm^{-1}. The solid line is a linear best fit. Right: Plot of oscillation period against cell length, for fixed MinD and MinE concentrations. Below bacterial lengths of 1.2 μm, oscillation is not observed.

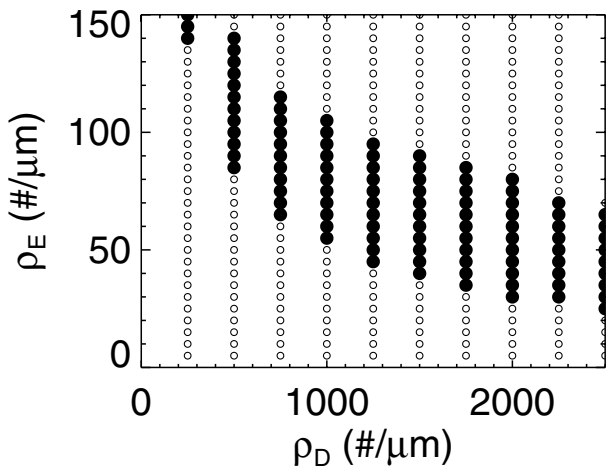

FIG. 4. Filled circles indicate regions of linear instability vs the density of MinD and MinE, where small inhomogeneities grew into a periodically oscillating pattern. Open circles indicate regions of linear stability where small inhomogeneities decay into a uniform and static pattern.

occur in bacteria of normal lengths and proper division regulation would be inhibited.

If the MinD concentration is increased or decreased beyond the limits shown in Fig. 3 (left), then the oscillation amplitude decays, and a uniform steady state results. The stability is mapped out in Fig. 4, as a function of protein concentration. This is consistent with experiment, where overexpression of MinD suppresses division [9]. Although varying the MinE concentration does affect the region of oscillatory instability (as shown in Fig. 4), it did not have a significant effect on the oscillation period. This appears somewhat contrary to the results of Ref. [3], possibly due to the absence of MinE dimerization in our model [20].

In conclusion, we have introduced a particle-conserving reaction-diffusion model that self-organizes to form a key regulatory mechanism for accurate midcell division site selection in *E. coli*. The model qualitatively agrees with many of the features found in experiments, and, in particular, naturally accounts for the oscillatory patterns of the *min* proteins. Already, our model leads us to make a number of striking predictions: We require that cytoplasmic MinD recruits MinE to the membrane; we require that the membrane-associated diffusion constants for MinD and MinE are very much less than their corresponding values in the cytoplasm; and we have mapped out the shape of the oscillation regime as a function of average MinD and MinE concentration.

Experimental characterization of reaction rates and diffusion constants do not yet severely constrain our model. Accurate experimental measurements of oscillation periods and wavelengths as a function of concentrations of MinD and MinE will provide a stringent test. There is also considerable scope for extending our results. In subsequent studies, we will explore a bulk $3d$ system with discrete particle dynamics and microscopic interactions between individual protein molecules. This will allow us to explicitly consider the influence of fluctuations due to discrete particles, the role of ATPase activity of MinD [17], and the effects of MinE dimerization [20].

This work was supported financially by NSERC Canada. We would like to thank Russell Bishop for encouragement and useful comments and Michael Greenwood for his development of imaging software.

*Current address: Instituut-Lorentz, Leiden University, P.O. Box 9506, 2300 RA Leiden, The Netherlands.

[1] N. Maki *et al.,* J. Bacteriol. **182**, 4337 (2000).
[2] K. P. Lemon and A. D. Grossman, Science **282**, 1516 (1998).
[3] D. M. Raskin and P. A. J. de Boer, Proc. Natl. Acad. Sci. U.S.A. **96**, 4971 (1999).
[4] D. M. Raskin and P. A. J. de Boer, J. Bacteriol. **181**, 6419 (1999).
[5] Z. Hu and J. Lutkenhaus, Mol. Microbiol. **34**, 82 (1999).
[6] S. L. Rowland *et al.,* J. Bacteriol. **182**, 613 (2000).
[7] X. Fu *et al.,* Proc. Natl. Acad. Sci. U.S.A. **98**, 980 (2001).
[8] C. A. Hale, H. Meinhardt, and P. A. J. de Boer, EMBO J. **20**, 1563 (2001).
[9] P. A. J. de Boer, R. E. Crossley, and L. I. Rothfield, Cell **56**, 641 (1989).
[10] L. Rothfield, S. Justice, and J. García-Lara, Annu. Rev. Genet. **33**, 423 (1999).
[11] X.-C. Yu and W. Margolin, Mol. Microbiol. **32**, 315 (1999).
[12] J. Huang, C. Cao, and J. Lutkenhaus, J. Bacteriol. **178**, 5080 (1996).
[13] L. I. Rothfield and C.-R. Zhao, Cell **84**, 183 (1996).
[14] M. C. Cross and P. C. Hohenberg, Rev. Mod. Phys. **65**, 851 (1993).
[15] J. D. Murray, *Mathematical Biology* (Springer-Verlag, Berlin, 1993), 2nd ed.
[16] H. Meinhardt, *Models of Biological Pattern Formation* (Academic Press, London, 1982).
[17] P. A. J. de Boer *et al.,* EMBO J. **10**, 4371 (1991).
[18] C.-R. Zhao, P. A. J. de Boer, and L. I. Rothfield, Proc. Natl. Acad. Sci. U.S.A. **92**, 4313 (1995).
[19] M. B. Elowitz *et al.,* J. Bacteriol. **181**, 197 (1999).
[20] G. F. King *et al.,* Mol. Microbiol. **31**, 1161 (1999).

Dynamic structures in *Escherichia coli*: Spontaneous formation of MinE rings and MinD polar zones

Kerwyn Casey Huang*†‡, Yigal Meir†§, and Ned S. Wingreen†

*Department of Physics, Massachusetts Institute of Technology, 77 Massachusetts Avenue, Room 12-111, Cambridge, MA 02139; †NEC Laboratories America, Incorporated, 4 Independence Way, Princeton, NJ 08540; and §Department of Physics, Ben Gurion University, Beer Sheva 84105, Israel

Communicated by Sydney Kustu, University of California, Berkeley, CA, August 25, 2003 (received for review June 26, 2003)

In *Escherichia coli*, division site selection is regulated in part by the Min-protein system. Oscillations of the Min proteins from pole to pole every ≈40 sec have been revealed by *in vivo* studies of GFP fusions. The dynamic oscillatory structures produced by the Min proteins, including a ring of MinE protein, compact polar zones of MinD, and zebra-striped oscillations in filamentous cells, remain unexplained. We show that the Min oscillations, including mutant phenotypes, can be accounted for by *in vitro*-observed interactions involving MinD and MinE, with a crucial role played by the rate of nucleotide exchange. Recent discoveries suggest that protein oscillations may play a general role in proper chromosome and plasmid partitioning.

In *Escherichia coli*, two systems are known to regulate the placement of the division site: nucleoid occlusion (1, 2) and the Min proteins (3). Both systems interfere with the formation of a ring of FtsZ protein believed to define the division site. The three Min proteins, MinC, MinD, and MinE, are required to prevent minicelling (3), asymmetric cell divisions that produce one small daughter cell lacking a chromosome and hence nonviable. In contrast, overexpression of MinC results in filamentous growth (4) by inhibiting polymerization of FtsZ on the cell membrane (5), a necessary first step in cell division (6). MinC is recruited to the membrane by MinD (7), which is membrane-associated only in its ATP-bound form (MinD:ATP) (8). Like MinC, MinE is naturally cytoplasmic and is recruited to the membrane by MinD:ATP (8).

In vivo observations of GFP fusions in living cells reveal spatial oscillations of the three Min proteins (9–11). In each oscillation period, the cell's entire complement of MinD accumulates in the cell membrane in a "polar zone" at one end of the cell. This polar zone then shrinks toward the end of the cell as a new accumulation forms at the opposite pole. MinC follows the same pattern as MinD, and the two proteins form complexes on the membrane. In contrast, MinE forms a ring at the boundary of the MinD polar zone with some MinE dispersed throughout the polar zone. The MinE ring moves toward the end of the cell as the MinD polar zone shrinks. The oscillation period is approximately proportional to the amount of MinD and inversely proportional to the amount of MinE in the cell, with a minimum period of ≈30 sec (9). Both MinD and MinE, but not MinC, are required for oscillations (9).

The average spatial distribution of the Min proteins naturally prevents minicelling without blocking normal cell division. The polar zones of MinD and MinC are believed to block FtsZ ring formation at the ends of the cell. At the same time, the concentrations of MinD and MinC remain low near the center of the cell, so an FtsZ ring can form there to establish the site of cell division.

Several models have been put forward to account for Min protein oscillations. All of these models successfully generate oscillations, but none can be meaningfully compared with *in vivo* observations. The model of Meinhardt and de Boer (12) requires newly synthesized protein to form both the MinD polar zones and MinE ring, because the proteins disappear (are degraded?) from the simulation on dissociation from the membrane. However, Min oscillations have been observed to persist for at least 45 min after protein synthesis was blocked, demonstrating Min-protein stability. Furthermore, to obtain a MinE ring, the Meinhardt and de Boer model assumes ad hoc that MinE attaches preferentially to an intermediate concentration of MinD.

The model of Howard, Rutenberg, and de Vet (HRdV) (13) produces oscillations only if MinE is driven onto the membrane by cytoplasmic MinD, despite evidence that MinE is recruited to the membrane by membrane-associated MinD (8). Moreover, the oscillations in the HRdV model have the opposite dependence of frequency on MinD concentration than is observed, and MinD forms a medial band that moves toward the end of the cell, contrary to the experimental observation that MinD forms directly as a polar zone. The model of Kruse (14) avoids ad hoc assumptions and produces a MinD polar zone by a MinD concentration-dependent slowing of MinD diffusion on the membrane, a natural assumption in light of recent experimental evidence for MinD polymer formation (8). However, the Kruse model requires unrealistically rapid membrane diffusion of MinD and fails to produce a MinE ring without ad hoc modification.

A Model Using Only Reported *in Vitro* Molecular Interactions Leads to Oscillations

Here we show that a model including only the reported *in vitro* interactions of MinD and MinE can fully account for the Min oscillations, including formation of compact MinD polar zones and a MinE ring. The specific interactions are shown schematically in Fig. 1. The oscillations are driven by a cycle in which MinD:ATP first associates with the membrane, preferentially where other MinD:ATP is located. MinE then attaches to the MinD:ATP, activates ATP hydrolysis, and MinE and MinD:ADP reenter the cytoplasm in a 1:1 ratio. Evidence for this cycle comes from *in vitro* experiments by Lutkenhaus and colleagues (8). In particular, MinD bound to ATP reshapes spherical phospholipid vesicles into tubes by forming helical polymers, demonstrating self-association of membrane-bound MinD:ATP. Moreover, MinE cosediments with MinD in the membrane and activates hydrolysis and disassembly of MinD polymers (8). Recent *in vivo* experiments by Rothfield and colleagues (15) also indicate formation of MinD polymers on the membrane.

Reaction–Diffusion Equations

The equations describing the time evolution of MinD and MinE concentrations in a cylindrical cell (see schematic of reaction cycle in Fig. 1) are

$$\frac{\partial \rho_{D:\mathrm{ADP}}}{\partial t} = \mathcal{D}_D \nabla^2 \rho_{D:\mathrm{ADP}} - \sigma_D^{\mathrm{ADP}\to\mathrm{ATP}} \rho_{D:\mathrm{ADP}} + \delta(r-R)\sigma_{de}\rho_{de} \quad [1]$$

‡To whom correspondence should be addressed. E-mail: kch23@mit.edu.

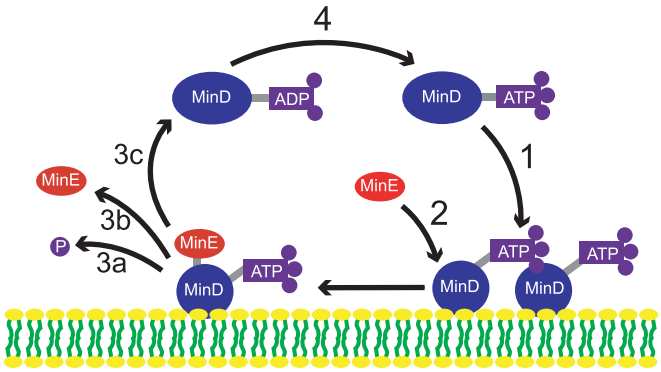

Fig. 1. Model MinD,E cycle driven by ATP hydrolysis. 1, Cytoplasmic MinD:ATP complex attaches to the membrane, preferentially where other MinD:ATP is bound. 2, MinE in the cytoplasm attaches to a membrane-associated MinD:ATP complex. 3, MinE activates ATP hydrolysis by MinD, breaking apart the complex and releasing phosphate (a), MinE (b), and MinD:ADP (c) into the cytoplasm. 4, MinD:ADP is converted back into MinD:ATP by nucleotide exchange. In wild-type cells, MinE is likely active as a homodimer (25).

$$\frac{\partial \rho_{D:\mathrm{ATP}}}{\partial t} = \mathcal{D}_D \nabla^2 \rho_{D:\mathrm{ATP}} + \sigma_D^{\mathrm{ADP}\to\mathrm{ATP}} \rho_{D:\mathrm{ADP}} - \delta(r-R)[\sigma_D + \sigma_{dD}(\rho_d + \rho_{de})]\rho_{D:\mathrm{ATP}} \quad [2]$$

$$\frac{\partial \rho_E}{\partial t} = \mathcal{D}_E \nabla^2 \rho_E + \delta(r-R)\sigma_{de}\rho_{de} - \delta(r-R)\sigma_E \rho_d \rho_E \quad [3]$$

$$\frac{\partial \rho_d}{\partial t} = -\sigma_E \rho_d \rho_E(R) + [\sigma_D + \sigma_{dD}(\rho_d + \rho_{de})]\rho_{D:\mathrm{ATP}}(R) \quad [4]$$

$$\frac{\partial \rho_{de}}{\partial t} = -\sigma_{de}\rho_{de} + \sigma_E \rho_d \rho_E(R), \quad [5]$$

where $\rho_{D:\mathrm{ADP}}$, $\rho_{D:\mathrm{ATP}}$, ρ_E are the concentrations in the cytoplasm of MinD:ADP complexes, MinD:ATP complexes, and MinE, and ρ_d, ρ_{de} are the concentrations on the membrane of MinD:ATP complexes and MinE:MinD:ATP complexes. We have verified that introducing an intermediate free cytoplasmic MinD species, thereby converting the single rate constant $\sigma_D^{\mathrm{ADP}\to\mathrm{ATP}}$ into two sequential decay rates, does not introduce any significant changes.

The cell radius is $R = 0.5$ μm, and results are given for cells of length $L = 4$ μm and 10 μm. The δ functions, $\delta(r - R)$, represent local exchange of proteins between membrane and cytoplasm; additional δ functions, $\delta(z)$ and $\delta(z - L)$, are implemented for the end caps of the cylinder. The total concentrations of MinD and MinE are 1,000/μm and 350/μm, respectively (assuming MinE is active as a homodimer, this implies 700 monomers per μm) (16). The diffusion constants are

$$\mathcal{D}_D = \mathcal{D}_E = 2.5\,\mu\mathrm{m}^2/\mathrm{sec},$$

as measured for the cytoplasmic diffusion of a maltose-binding protein in the *E. coli* cytoplasm (17), and the reaction rates are

$$\sigma_D^{\mathrm{ADP}\to\mathrm{ATP}} = 1/\mathrm{sec}, \quad \sigma_D = 0.025\ \mu\mathrm{m/sec},$$

$$\sigma_{dD} = 0.0015\ \mu\mathrm{m}^3/\mathrm{sec},$$

$$\sigma_{de} = 0.7/\mathrm{sec}, \quad \sigma_E = 0.093\ \mu\mathrm{m}^3/\mathrm{sec},$$

unless otherwise indicated. We discretize and solve Eqs. **1**–**5** on a 3D lattice in cylindrical coordinates, with grid spacing $dr = dz = 0.05$ μm.

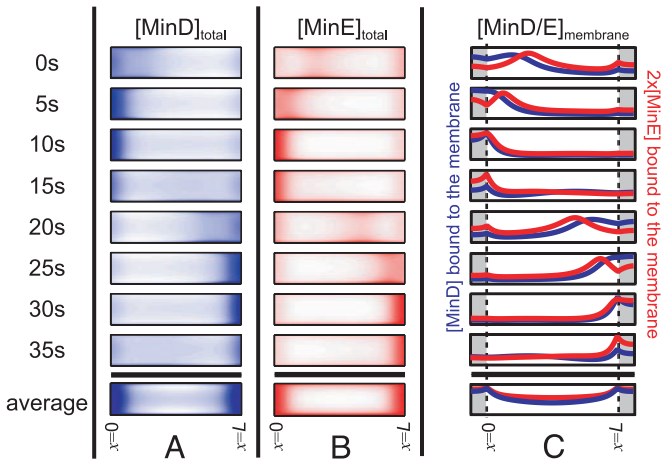

Fig. 2. Time slices in 5-sec increments of one complete MinD, MinE oscillation in a 4-μm cell. To mimic experimental observations of GFP fluorescence, we show 2D projections of the concentrations of MinD (*A*) and MinE (*B*) inside a 3D cylindrical cell, with the concentrations assumed rotationally symmetric about the axis of the cylinder. In *A*, the MinD polar zone shrinks toward the end of the cell and reforms at the opposite pole. In *B*, MinE forms a ring near the boundary of the MinD polar zone. Except during brief cytoplasmic-burst phases (15 sec, 35 sec), both MinD and MinE are primarily membrane-bound. (*C*) The membrane-associated concentrations, MinD:ATP in blue and MinE in red. The vertical dashed lines and gray shading indicate the caps of the cylindrical cell membrane. The final row shows the time average of each quantity over a complete cycle.

Periodic Oscillations with MinD Polar Zones and a MinE Ring

The results of numerical integration in time of our model equations (see Fig. 1) for a 4-μm cylindrical cell are shown in Fig. 2. Periodic oscillations that are independent of initial conditions occur for a wide range of parameters. The oscillations have the same spatial character as those observed in experiment, including the formation and shrinkage of the MinD polar zones and the appearance of a MinE ring. These structures form spontaneously without special targets for MinD at the cell ends, without MinE–MinE interactions, and with no new protein synthesis. MinD:ATP and MinE dwell in one-half of the cell membrane during a period of polar zone compaction, before a brief cytoplasmic burst results in rapid reformation of a new MinD polar zone and MinE ring at the opposite end of the cell. The bottom row of Fig. 2 shows the time-averaged concentrations

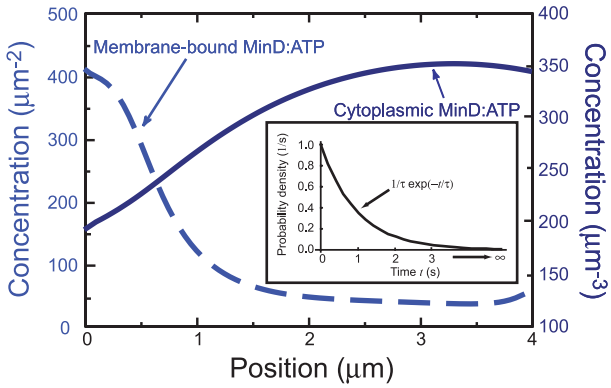

Fig. 3. Concentration of ATP-bound MinD (MinD:ATP) in the cytoplasm corresponding to time $t = 5$ sec in Fig. 2. The distribution is peaked at the opposite end of the cell from the existing MinD:ATP polar zone, indicated by the peak of the dashed curve, leading to the accumulation of MinD:ATP in a new polar zone. (*Inset*) Waiting-time distribution for recovery of MinD:ATP, assuming a nucleotide-exchange rate $1/\tau = \sigma_D^{\mathrm{ADP}\to\mathrm{ATP}}$ of 1/sec.

CELL BIOLOGY

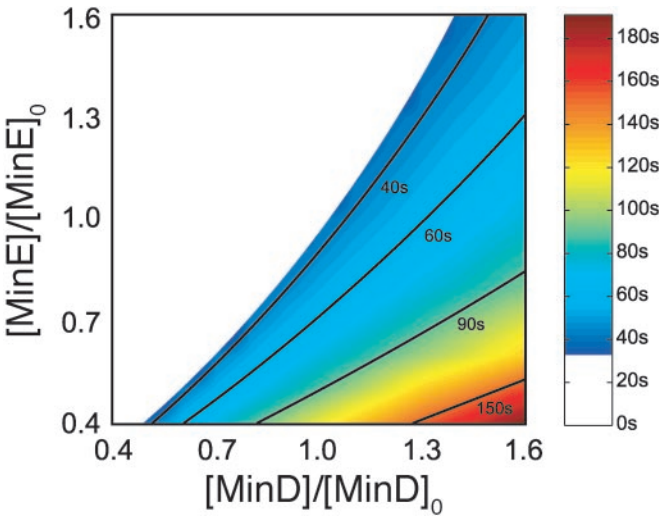

Fig. 4. Dependence of the oscillation period on the average concentration of MinD and MinE in a 4-μm cell. Wild-type values are $[MinD]_0 \approx 1{,}000/\mu m$ and $[MinE]_0 \approx 350/\mu m$, respectively (16). Isoperiod curves from 40 s to 150 s are shown.

of MinD and MinE. The minimum for membrane-bound MinD:ATP occurs at the center of the cell.

The basic mechanism of the oscillations is that a typical MinD, once released from the membrane, diffuses farther in the cytoplasm than does a typical MinE before reattaching to the membrane. The delay before MinD becomes competent to reattach to the membrane stems from its need to release ADP and rebind ATP, allowing the formation of a new polar zone of MinD:ATP, whereas MinE progressively hydrolyzes the old polar zone.

But why does MinD:ATP accumulate at the far pole rather than reattaching uniformly throughout the cell? The reason is that MinD:ATP in the cytoplasm sticks rapidly to the old polar zone from which it was released. Indeed, a MinD protein typically recycles ≈4 times through the old polar zone in each half cycle before finally lodging in the new polar zone. Each such recycling of MinD requires the hydrolysis of one molecule of ATP. The "stickiness" of the old polar zone creates a distribution of MinD:ATP in the cytoplasm that is peaked at the opposite end of the cell (Fig. 3). Thus MinD:ATP accumulates in a new polar zone, with a profile sharpened by the tendency of MinD:ATP in the membrane to self-associate (8).

Proper formation of the new MinD:ATP polar zone requires that MinD have time to diffuse throughout the cytoplasm before rebinding ATP. The nucleotide exchange rate we use, $\sigma_D^{ADP \to ATP}$ = 1/sec, is well within the observed range, which is known to span more than five orders of magnitude for guanine nucleotide exchange (18). If the exchange rate is too large, cytoplasmic MinD:ATP reappears mainly near the old polar zone, eliminating the peaked distribution of cytoplasmic MinD:ATP (Fig. 3) that is responsible for the formation of a new polar zone. The delay of MinD:ATP recovery due to nucleotide exchange has been ignored in previous models.

Once MinE completes the hydrolysis of the old polar zone, it begins to diffuse through the cytoplasm. Because MinE sticks rapidly to available MinD:ATP in the membrane, most of the MinE attaches to the edge of the new MinD:ATP polar zone. This is the origin of the MinE ring. The subsequent movement of the MinE ring toward the end of the cell reflects release from the membrane, diffusion, and reattachment of individual MinE molecules (or homodimers). Because the diffusion length of MinE before reattaching is generally smaller than the ≈1 μm transverse dimension of the cell, it is important to model the oscillations in a fully 3D cell rather than in a 1D approximation as used in the models from refs. 12–14. We neglect membrane diffusion as too slow to affect the dynamics of the oscillations.

The Oscillation Period Depends Linearly on the Ratio of MinD to MinE Concentration

Fig. 4 shows the period of oscillation for a range of protein concentrations. Consistent with experiment (9), the oscillation period is proportional to the total amount of MinD and inversely proportional to the total amount of MinE in the cell. The period is simply determined by the rate at which the MinE ring hydrolyzes the polar zone of MinD:ATP. This period increases almost linearly with the amount of MinD in the cell and decreases inversely with both the amount of MinE and the hydrolysis rate σ_{de}. We chose σ_{de} = 0.7/sec to match the observed wild-type period of ≈40 sec (9). Varying the total amounts of MinD and MinE in the cell, we find a minimum oscillation period of ≈33 sec, also consistent with experiment (9). Increasing the amount of MinE beyond this limit forces a majority of the MinD into the cytoplasm and eliminates oscillations. In contrast, decreasing the concentration of MinE results in slower and slower oscillations with no apparent limit, consistent with *in vivo* observations (9).

Filamentous Cells Have "Doubled" Oscillation Patterns

A critical test of the model is the striking behavior of Min oscillations in long cells. Filamentous cells can be obtained by using temperature-sensitive FtsZ mutants, which cannot undergo cell division at the nonpermissive temperature. For cells longer than ≈10 μm, the number of wavelengths of Min oscillations present in the cell increases; zebra-striped cells with as many as eight half-wavelengths have been observed (9). Fig. 5 shows the oscillation pattern obtained from our model for a

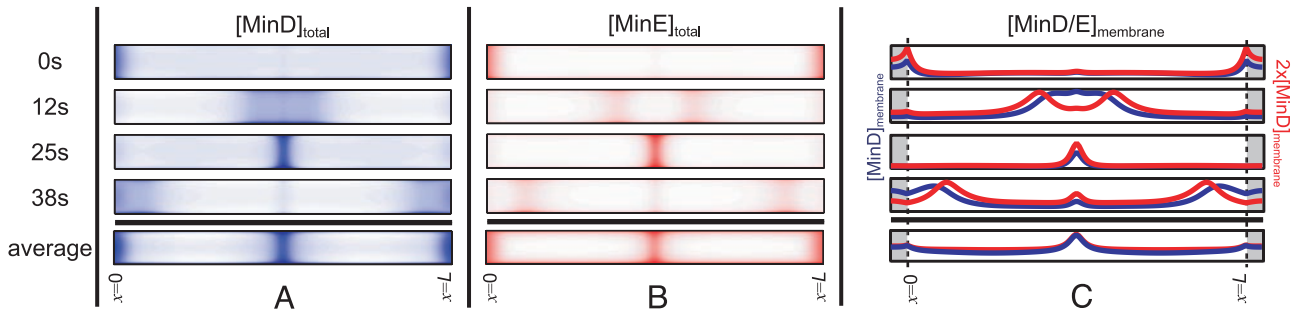

Fig. 5. Time slices in 12.5-sec increments of one complete MinD, MinE oscillation in a 10-μm cell. The same quantities are shown as in Fig. 2. The zebra-striped oscillation pattern now includes two half-wavelengths. The system exhibits two separate MinE rings and an alternation between two MinD polar zones and a central MinD tube. The final row shows the time average of each quantity over a complete cycle.

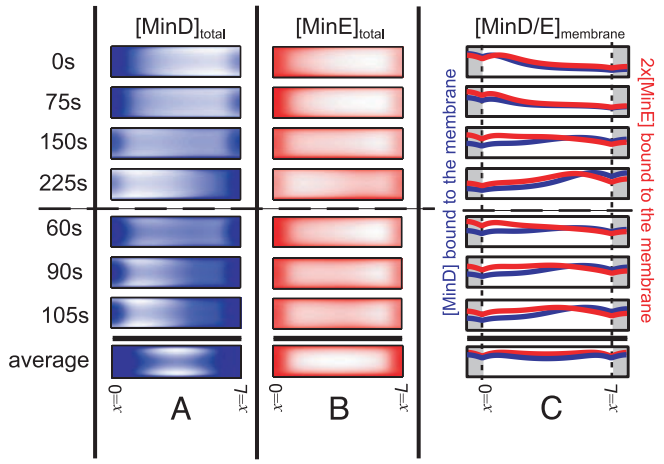

Fig. 6. An oscillation period for a "MinE mutant" with reduced hydrolysis rate, $\sigma_{de} = 0.07$/sec, and reduced MinE sticking coefficient, $\sigma_E = 0.047$ μm/sec. The upper half portrays time slices of half an oscillation cycle in 75-sec increments, whereas the lower half focuses on the time interval from 60 to 105 sec, during which the MinE finishes hydrolyzing the old MinD polar zone, diffuses across the cell, and reforms on the opposite half. The same quantities are shown as in Fig. 2. Note the long oscillation period and the suppression of a MinE ring.

10-μm cell. Consistent with experimental observations, the oscillation pattern "doubles;" the oscillatory dynamics in each half of the cell mimics the dynamics of the normal 4-μm cell in Fig. 2. We find that this doubled oscillation pattern is stable for a 3D cell but collapses back to an undoubled pattern (Fig. 2) in the 1D approximation. In addition, a nucleotide exchange rate of $\approx$1/sec or slower is necessary for stability of the doubled oscillation pattern. The bottom row of Fig. 5 shows the time-averaged concentrations of MinD and MinE. The minima for membrane-bound MinD:ATP occur at 1/4 and 3/4 of the cell length, as observed by Gullbrand and Nordström (19) for FtsZ ring placement in long cells. Oscillations in a 20-μm cell closely correspond to a "doubled" 10-μm cell (not shown).

MinE "Mutants": Slow Oscillations and No MinE Ring Formation

Another striking experimental observation is that cells with the wild-type $MinE^{1-88}$ protein replaced by the fragment $MinE^{1-53}$ display oscillations with a period of $\approx$10 min with no detectable MinE ring and with diffuse MinD polar zones (20). Recent experiments with MinE mutants have correlated a weak or absent MinE ring with extended MinD polar zones and an increased minicelling probability (16). Within our model, the oscillation period varies inversely with the hydrolysis rate σ_{de}, and ring formation depends on the attachment probability of MinE to available MinD:ATP in the membrane. In Fig. 6, we show oscillations of MinD and MinE with a reduced hydrolysis rate, $\sigma_{de} = 0.07$/sec, which slows the oscillations, and a reduced MinE attachment coefficient $\sigma_E = 0.047$ μm/sec. With this value of σ_E, the MinE ring fails to form, because MinE diffuses well into the new polar zone before reattaching to MinD:ATP (increasing the MinE diffusion constant has a similar effect). Importantly, this invasion of the MinD:ATP polar zone by MinE results in less accumulation of MinD:ATP and a more diffuse MinD:ATP polar zone, similar to experimental observations.

Discussion

Some aspects of Min protein oscillations are not captured by our minimal model. For example, the MinE ring is occasionally observed to reverse direction or "stutter" (16), likely reflecting the persistent presence of helical accumulations of MinD (15). Although the model cannot predict the fine structure of MinD polymerization (15), nevertheless, the agreement between model and experiment is close enough to indicate some fundamental properties of the real Min system. The model oscillations represent a limit cycle; that is, the same oscillation develops from any set of initial conditions. Moreover, the pattern of oscillation, particularly the formation of compact polar zones of MinD:ATP capped by a ring of MinE, is insensitive to fluctuations in the amounts of MinD and MinE. A linear-stability analysis around the uniform solution yields instability only for half-wavelengths >2 μm. This minimum wavelength guarantees that oscillations can develop only in the cell's long dimension. Interestingly, the period of oscillations is sensitive to protein number fluctuations (Fig. 4), but periods of up to $\approx$120 sec (9) appear to yield a normal division phenotype.

Recent observations suggest a general role for protein oscillators in chromosome and plasmid partitioning (21, 22). Nevertheless, it remains an open question why bacteria use such oscillators. The Gram-positive bacterium *Bacillus subtilis* uses homologs to MinC and MinD to prevent minicelling. However, these proteins form static polar zones in *B. subtilis*. (*B. subtilis* also undergoes highly asymmetric cell division during sporulation.) In the absence of Min proteins in *E. coli*, nucleoid occlusion results in division sites either near the cell ends, resulting in minicelling, or medially, resulting in essentially normal divisions, but with considerably less division accuracy than in wild type (2). In anucleate cells without nucleoid occlusion but with Min proteins, medial FtsZ ring placement is favored but again with less accuracy than in wild type (2). It is unknown whether Min protein oscillations alone can be sufficient for accurate FtsZ ring placement, or whether cooperation and possibly direct interaction between the Min system and nucleoid occlusion are required. In *B. subtilis*, the nonoscillatory MinCD homologs are not required for medial division accuracy (23). One possible advantage of an oscillator for determining the cell center is that in each half cycle, essentially the same amount of MinD protein accumulates in each polar zone. Thus, the time-averaged minimum of MinD, and hence the minimum of the division-site blocker MinC, will occur at the cell center independent of protein number fluctuations. Furthermore, recent indications (24) that MinC and MinE may competitively bind to MinD and that MinD forms dimers in the cytoplasm may enhance the FtsZ ring placement accuracy of the Min oscillator. Finally, the observation of FtsZ ring formation at the 1/4 and 3/4 points in long cells (19) very likely reflects the doubling of the Min-oscillation pattern. The multiwavelength Min oscillations in long cells may play a role in proper fragmentation and reduce the likelihood of internal minicelling during recovery from filamentous growth induced by the SOS response.

We thank Joe Lutkenhaus for valuable suggestions and Bonnie Bassler, Laura Garwin, and Tom Silhavy for critical readings of the manuscript. Partial funding for this research was provided by the Materials Research Science and Engineering Centers Program of the National Science Foundation under Grant DMR-0213282.

1. Woldringh, C. L., Mulder, E., Valkenburg, J. A., Wientjes, F. B., Zaritsky, A. & Nanninga, N. (1990) *Res. Microbiol.* **141,** 39–49.
2. Yu, X.-C. & Margolin, W. (1999) *Mol. Microbiol.* **32,** 315–326.
3. de Boer, P. A. J., Crossley, R. E. & Rothfield, L. I. (1989) *Cell* **56,** 641–649.
4. de Boer, P. A. J., Crossley, R. E. & Rothfield, L. I. (1992) *J. Bacteriol.* **174,** 63–70.
5. Bi, E. & Lutkenhaus, J. (1993) *J. Bacteriol.* **175,** 1118–1125.
6. Bi, E. & Lutkenhaus, J. (1991) *Nature* **354,** 161–164.
7. Huang, J., Cao, C. & Lutkenhaus, J. (1996) *J. Bacteriol.* **178,** 5080–5085.
8. Hu, Z., Gogol, E. P. & Lutkenhaus, J. (2002) *Proc. Natl. Acad. Sci. USA* **99,** 6761–6766.

9. Raskin, D. M. & de Boer, P. A. J. (1999) *Proc. Natl. Acad. Sci. USA* **96,** 4971–4976.
10. Hu, Z. & Lutkenhaus, J. (1999) *Mol. Microbiol.* **34,** 82–90.
11. Fu, X., Shih, Y.-L., Zhang, Y. & Rothfield, L. I. (2001) *Proc. Natl. Acad. Sci. USA* **98,** 980–985.
12. Meinhardt, H. & de Boer, P. A. J. (2001) *Proc. Natl. Acad. Sci. USA* **98,** 14202–14207.
13. Howard, M., Rutenberg, A. D. & de Vet, S. (2001) *Phys. Rev. Lett.* **87,** 278102-1–278102-4.
14. Kruse, K. (2002) *Biophys. J.* **82,** 618–627.
15. Shih, Y.-L., Le, T. & Rothfield, L. (2003) *Proc. Natl. Acad. Sci. USA* **100,** 7865–7870.
16. Shih, Y.-L., Fu, X., King, G. F., Le, T. & Rothfield, L. (2002) *EMBO J.* **21,** 3347–3357.
17. Elowitz, M. B., Surette, M. G., Wolf, P.-E., Stock, J. B. & Leibler, S. (1998) *J. Bacteriol.* **181,** 197–203.
18. Lenzen, C., Cool, R. H., Prinz, H., Kuhlmann, J. & Wittinghofer, A. (1998) *Biochemistry* **37,** 7420–7430.
19. Gullbrand, B. & Nordström, K. (2000) *Mol. Microbiol.* **36,** 1349–1359.
20. Rowland, S. L., Fu, X., Sayed, M. A., Zhang, Y., Cook, W. R. & Rothfield, L. I. (2000) *J. Bacteriol.* **182,** 613–619.
21. Yamaichi, Y. & Niki, H. (2000) *Proc. Natl. Acad. Sci. USA* **97,** 14656–14661.
22. Ebersbach, G. & Gerdes, K. (2001) *Proc. Natl. Acad. Sci. USA* **98,** 15078–15083.
23. Migocki, M. D., Freeman, M. K., Wake, R. G. & Harry, E. J. (2002) *EMBO Rep.* **3,** 1163–1167.
24. Hu, Z., Saez, C. & Lutkenhaus, J. (2003) *J. Bacteriol.* **185,** 196–203.
25. Pichoff, S., Vollrath, B., Touriol, C. & Bouché, J.-P. (1995) *Mol. Microbiol.* **18,** 321–329.